Universiteit Leiden
The Netherlands

Transduction patterns in the CNS following various routes of AAV-5-mediated gene delivery

Pietersz, K.L.; Martier, R.M.; Baatje, M.S.; Liefhebber, J.M.; Brouwers, C.C.; Pouw, S.M.; ... ; Blits, B.

ARTICLE

Transduction patterns in the CNS following various routes of AAV-5-mediated gene delivery

K. L. Pietersz[1,2] · R. M. Martier[1,3] · M. S. Baatje[1] · J. M. Liefhebber[1] · C. C. Brouwers[1] · S. M. Pouw[1] · L. Fokkert[1] · J. Lubelski[1] · H. Petry[1] · G. J. M. Martens[2] · S. J. van Deventer[1,3] · P. Konstantinova [ID][1] · B. Blits[1,4]

Abstract
Various administration routes of adeno-associated virus (AAV)-based gene therapy have been examined to target the central nervous system to answer the question what the most optimal delivery route is for treatment of the brain with certain indications. In this study, we evaluated AAV5 vector system for its capability to target the central nervous system via intrastriatal, intrathalamic or intracerebroventricular delivery routes in rats. AAV5 is an ideal candidate for gene therapy because of its relatively low level of existing neutralizing antibodies compared to other serotypes, and its broad tissue and cell tropism. Intrastriatal administration of AAV5-GFP resulted in centralized localized vector distribution and expression in the frontal part of the brain. Intrathalamic injection showed transduction and gradient expression from the rostral brain into lumbar spinal cord, while intracerebroventricular administration led to a more evenly, albeit relatively superficially distributed, transduction and expression throughout the central nervous system. To visualize the differences between localized and intra-cerebral spinal fluid administration routes, we compared intrastriatal to intracerebroventricular and intrathecal administration of AAV5-GFP. Together, our results demonstrate that for efficient transgene expression, various administration routes can be applied.

Introduction

Since the first clinical protocol was published for the treatment of Canavan's disease (CD) in 2002 [1] great progress has been made in the field of adeno-associated virus (AAV) for neurological diseases. Long-term follow-up

These authors contributed equally: K. L. Pietersz, R. M. Martier

✉ P. Konstantinova
P.konstantinova@uniqure.com

1 Department of Research & Development, uniQure biopharma B.V., Amsterdam, the Netherlands

2 Department of Molecular Animal Physiology, Donders Institute for Brain, Cognition and Behaviour, Centre for Neuroscience, Faculty of Science, Radboud University, Nijmegen, the Netherlands

3 Department of Gastroenterology and Hepatology, Leiden University Medical Center, Leiden, the Netherlands

4 Present address: Blits Biopharma Consultancy and DegenRx BV, Amsterdam, the Netherlands

studies have shown that although intra-cortical administration of AAV2-based therapy was safe, no clear benefit of the therapy has been observed, most likely due to insufficient delivery and hence inadequate expression of the therapeutic gene at the correct location [1]. The 2002 clinical study has illustrated the importance of effective delivery to all affected sites. Cortical delivery of AAV2 resulted in relatively low transduction of tissue beyond the injection site. Therefore, other areas affected in CD, such as the brainstem and cerebellum, were not transduced. In addition, in the brain the substrate of the mutated enzyme is found mostly in oligodendrocytes and their progenitor cells with smaller amounts in microglia and brainstem neurons. As AAV2 predominantly transduces neurons, the affected cells are not targeted by this serotype.

AAV5 is an ideal candidate for gene therapy as it has relatively low seroprevalence, i.e., antibodies against the capsid, compared with other serotypes [2] and a broad tropism for muscle, liver, and CNS [3, 4]. Intrastriatal (IStr) delivery of AAV5 to the murine brain has resulted in high degree of transduction of the striatum when compared to AAV serotypes 1, 2, 4, 6, 8, and 9 [3]. IStr administration of AAV5 to rats [5] and primates [6, 7] showed improvement

in transgene expression with regards to expression levels and scope of target cell population for AAV5 compared to other serotypes tested. Furthermore, following IStr administration AAV5 is transduced into neurons, astrocytes, microglia, and oligodendrocytes [3] and into distant nuclei such as substantia nigra (SN) reticulata, globus pallidus, cortex, and thalamus of non-human primates [8]. In addition, recently we have shown that AAV5 is capable of transducing a broad range of human induced pluripotential central nervous system cells types, such as astrocytes, motor neurons, and dopaminergic neurons [9]. Thus, AAV5 is a promising vector for disease indications that require a global transduction of the brain.

AAV can be administered through various routes, e.g., directly into the parenchyma (brain or spinal cord), into the cerebrospinal fluid (CSF) or intravenously (IV), in an effort to specifically target affected sites, whereby each route has its characteristics with specific advantages and disadvantages. In human subjects, intrathecal (IT) delivery is a relatively non-invasive procedure consisting of a lumbar puncture. Schuster et al. [10] have shown that at the lumbar site IT administration of AAV5-GFP in mice led to GFP expression throughout the spinal cord and in discrete regions of the CNS throughout the rostro-caudal extent of the neuroaxis [8, 10]. Broader transduction of the rostral part of the brain may be achieved with an intracerebroventricular (ICV) injection into the lateral ventricle. Above mentioned studies have also shown that AAV5 does not cross the blood–brain barrier after intravenous delivery and hence this delivery route was not taken into consideration in the current study.

Different transduction patterns are desirable in order to target various diseases. For instance, in Parkinson's Disease (PD) neurodegeneration mainly occurs in dopaminergic cells of the SN [11], while prominent neuropathology in Huntington's Disease (HD) occurs within the striatal part of the basal ganglia, and secondary marked neuronal loss and shrinkage is observed in the deep layers of the cerebral cortex [12]. Parenchymal administration of AAV could result in significant transduction for production of therapeutic protein in these areas. In the monogenetic disease Niemann Pick Type C, a progressive loss of Purkinje cells is observed [13], the cerebellum and brainstem is the genesis of neuropathology in spinocerebellar ataxias, and the hippocampus is the earliest brain region affected in Alzheimer's Disease (AD). Direct administration of therapeutic-encoding AAV2/5 to the hippocampus in an AD model has been shown to ameliorate disease progression [14]. These studies make hippocampal and cerebellar transduction of interest for transgene delivery. In order to develop a therapy for these disorders, it is essential to characterize to what extent a transgene is

delivered by AAV to the brain or spinal cord. In some cases, a broader delivery spectrum may be needed, such as in patients with Amyotrophic Lateral Sclerosis where both the upper and lower motor neurons of the brain and spinal cord are affected. Another example is the neurological phenotype of infantile Pompe's disease where the brainstem motor and sensory neurons, spinal cord motor-, sensory-, and interneurons are affected [15]. For these indications, a broader transduction pattern seems necessary, e.g., via an intrathecal approach. Recently, a phase-1 trial for SanFilippo B disease has shown that 16 intraparenchymal injections of AAV2/5 encoding the deficient enzyme alpha-N-acetylglucosaminidase into white matter of the cortex were well tolerated [16]. Theoretically, by infusing into a more central area in the brain, it might be possible to reach the affected areas with one bilateral IStr or intrathalamic (ITH) administration. Both sites have multiple anterograde and retrograde projections throughout the brain. These projections can be used to predict and utilize the distribution of the transgene product. Moreover, the choice of serotype can also influence the expression pattern, expanding the possibilities and necessities of a so-called AAV toolbox even further.

In this study, we explored the transduction pattern of AAV5 following IStr, ITH, ICV, or IT administration. Predictable transduction patterns will aid the design of new therapeutic strategies.

Material and methods

Production of vectors

Vectors were produced using uniQure's patented insect cell-based system as previously described [17]. Briefly, Spodoptera Frugiperda (SF) + cells were infected with recombinant baculovirus encoding for the capsid AAV5, REP gene and insert. The expression cassette of the insert consisted of the nucleotides defining CAG promoter, a combination of the cytomegalovirus early enhancer element and chicken beta-actin promoter. The transgene GFP is preceded by a Kozak sequence and followed by the bovine growth hormone polyadenylation signal. Expression cassette is flanked by two inverted terminal repeats. At 72 h post triple-infection, cells were lysed and clarified lysate was purified on the AKTA explorer (FPLC chromatography system, GE healthcare) using AVB sepharose (GE healthcare). The vectors were titrated by Sybergreen Q-PCR using a primer pair binding to the promoter region (forward primer; GAG CCG CAG CCA TTG C, reverse primer; CAC AGA TTT GGG ACA AAG GAA GT) expressed as genome copies per ml (GC/ml).

Table 1 Overview of volume and dosages used in study.

Study	Injection route	Sample size	Volume (μl)	Total dose (GC/rat)	Titer (GC/ml)
Injection routes 1st study	IStr	3	2 (per hemisphere)	5×10^{10}	1.25×10^{13}
	ITH	3	2 (per hemisphere)		
	ICV	3	40	5×10^{11}	1.25×10^{13}
Injection routes 2nd study	IStr	3	1 (per hemisphere)	1×10^{11}	1×10^{14}
	ICV	3	50	5×10^{12}	1×10^{14}
	IT	3	50	5×10^{12}	1×10^{14}

Animal study

All animal studies described were approved by the local animal experimentation ethical committee. Young adult (150–180 g) female Wistar rats (Janvier labs) were used for all experiments. Animals were allocated to groups at random, as this study was not intended for quantitative analysis a minimum sample size of 3 was chosen. Rats were anesthetized before surgery, by intramuscular administration of Hypnorm/Dormicum. A small hole is drilled in the skull, and the striatum or lateral ventricle are stereotactically approached. Coordinates for IStr infusion were A/P 1.3, L+/- 2.5, and D 3.5; for ITH A/P -2.5, L ± 3 and D 4.5; for unilateral intracerebroventricular A/P -1.5, L 2.5, and D 3.5. For the IT administration, an incision was made in the skin on the back of the animal, muscle layers are split and a laminectomy performed at the lumbar vertebral level L3. The animal is placed into the spinal cord fixator, care was taken to only open the dura. A flexible guiding tube is inserted at the cervical level just below the dura, between dura and pia, pointing horizontally towards the lumbar area. Then, the tube is carefully pushed towards the lumbar area. When the tubing arrives at the thoracic level and some resistance is experienced, the tubing was not placed correctly. When it slides through, the location is correct and the dose is administered. Volumes and dosage are described in Table 1. After surgery, animals are given Temgesic for pain relief and returned to their cage. Depending on the experiment, 4 or 6 weeks after experiments animals were sacrificed by decapitation under isoflurane anesthesia. Brains were longitudinally cut in half to identify brain areas and care was given to peel off the cortex before dividing into smaller pieces. Organs used for distribution analysis were snap frozen in liquid nitrogen and stored at −80 °C until analysis. Brains used for histology were fixed in 4% paraformaldehyde for 24–48 h.

Vector distribution and GFP expression

Organs were retrieved from −80 °C and pulverized to a powder using the Cryoprep system (Covaris, Woburn, MA, USA), from ±10 mg powder DNA was extracted using the DNeasy 96 Blood and Tissue kit (QIAGEN, Germany). Vector DNA was detected by Q-PCR using TaqMan primers and probe binding to CAG promoter (forward primer: GAG CCG CAG CCA TTG C, reverse primer: CAC AGA TTT GGG ACA AAG GAA GT, probe: ATG GTA ATC GTG CGA GAG GGC GC). Vector DNA gc per μg DNA were quantified by interpolating from a standard line prepared from the plasmid of the expression cassette. RNA was isolated from powder using the RNeasy kit from Qiagen. Total RNA was reverse transcribed to cDNA using Maxima strand kit. RNA expression was quantified by using primers binding to GFP (forward primer: AGC AAA GAC CCC AAC GAG AA, reverse primer: GCG GCG GTC ACG AAC TC probe: CGC GAT CAC ATG GTC CTG CT) and GAPDH (Taqman expression array from Thermo Fisher) as housekeeping gene for reference. RNA expression was calculated using the ΔCT method normalized to the housekeeping gene. Investigators performed experiment blindly by coding samples.

Histology

24–48 h after immersion fixation in 4% paraformaldehyde brains were embedded in 10% gelatin (Difco) in PBS as described previously [18]. Embedded tissue was sectioned on a vibratome. Coronal sections were collected in PBS in series at a thickness of 50 μM. Immunohistochemistry was performed on free-floating sections. Endogenous peroxidase block was performed by incubating sections for 1 h in 1% H_2O_2/30% ethanol in PBS. Sections were washed three times with washing buffer (PBS/0,05% tween). A-specific blocking was performed by incubating sections for 1 h in PBS supplemented with 4% BSA (Bovine Serum Albumin) and 5% Normal Goat Serum (NGS). Subsequently, sections were incubated overnight with primary antibody against GFP (Abcam ab290), diluted 1:1000 in PBS/1%BSA/1.25%NGS/0.5% Tween and incubated for one hour with horse radish peroxidase-conjugated anti-rabbit before detection with 3,3'-Diaminobenzidine according to manufacturer's instructions (Dako envision kit K4009). Sections of the spinal cord were counterstained with haematoxylin and eosin stain (H&E). Subsequently, they were dehydrated
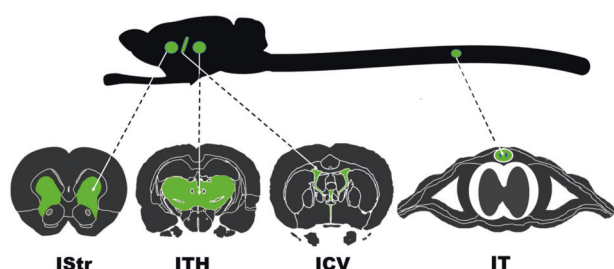
Fig. 1 Overview of injection routes. Intrastriatal (IStr), intrathalamic (ITH), intracerebroventricular (ICV), and intrathecal (IT) injections in the rat have been performed in this study. Green areas indicate the site of injection and the predicted spread of the fluid containing the vector.

through ethanol series, Xylene and embedded in Entellan before microscopical analysis. Investigators performed experiment blindly by coding samples.

Results

IStr, ICV, and ITH administration of AAV5 leads to distinct vector DNA distributions and transgene RNA expression patterns in rats

Presence of recombinant nucleic acids (DNA and RNA) was used to evaluate the capability of AAV5 to transduce the brain after parenchymal or CSF-mediated administration after AAV5 was administered to rats IStr, ICV, or ITH (Fig. 1). IStr injection of AAV5-GFP resulted in vector DNA and GFP RNA expression in the cortex, striatum, thalamus, and hippocampus (Fig. 2a brain). Vector DNA was not detected above background levels of PBS injected animals (1×10^3 genome copies (GC)/µg genomic DNA) in the cerebellum, brain stem, spinal cord, or peripheral organs (Fig. 2a).

ITH administration of AAV5-GFP led to the transduction (both presence of vector and GFP RNA expression) in the cortical-, striatal-, thalamic-, hippocampal-, cerebellar area, and brainstem (Fig. 2b, brain). Furthermore, we also observed vector DNA and GFP RNA presence in the spinal cord, albeit at a lower level than in the brain (Fig. 2b, spinal cord). Surprisingly, vector DNA was detected in the spleen. However, this did not result in GFP relative expression above background levels. (Fig. 2b peripheral organs).

ICV-administered rats showed a more evenly divided distribution pattern with similar amounts of vector DNA, and GFP RNA expression throughout the brain and spinal cord (Fig. 2c brain and spinal cord). Vector DNA was also retrieved in liver, kidney, and spleen (Fig. 2c peripheral organs). However, in the peripheral organs there was no GFP RNA detected above background levels, even though the CAG promoter is classified as a ubiquitous expression promoter [19].
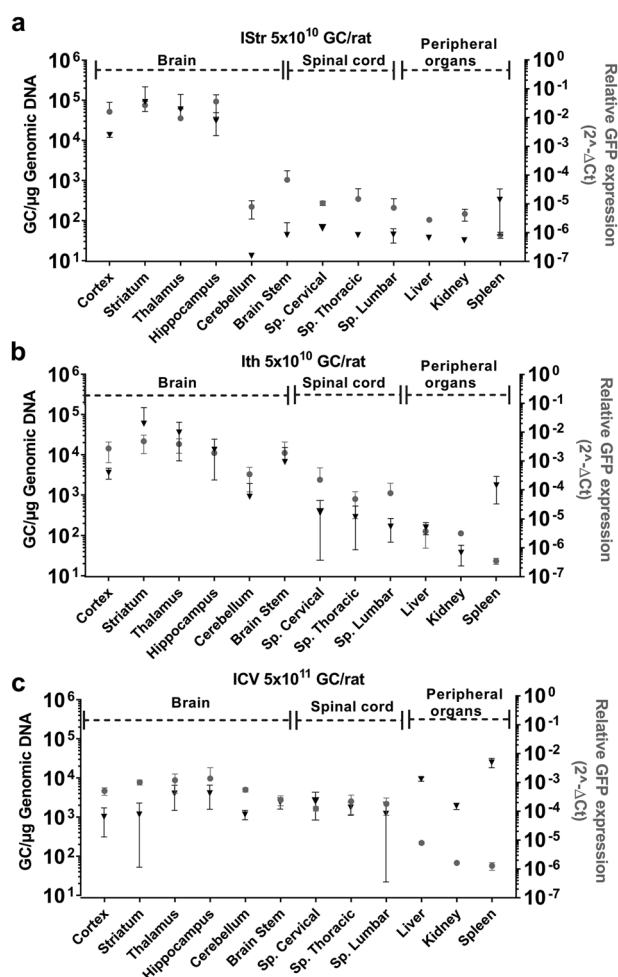

Fig. 2 Vector distribution and GFP expression following various cerebral administration routes of AAV5-GFP in rats. Rats ($n = 3$) received a total of 5E10 genomic copies (GC) of AAV5-CAG-GFP bilaterally by intrastriatal (IStr) (a), intrathalamic (ITH) (b), or 5E11GC total via Intracerebroventricular (ICV) (c) administration. Tissues were collected eight weeks post surgery, and DNA and RNA were isolated to determine the vector distribution and GFP expression. IS-administration results in distribution and expression in the frontal areas, basal ganglia, and midbrain. ITH-administration leads to a more spread gene expression compared to IStr-administration. Animals injected with PBS were used as negative control to determine background level of DNA (1×10^3 GC/µg DNA. Black triangles represent GC/µg genomic DNA, whereas gray circles represent relative GFP expression (RNA). Sp: spinal cord, error bars represent Standard deviation.

Distinct protein expression pattern observed at macro level when comparing IStr administration of AAV5-GFP to ICV and IT in rats

We delved further into the potential use of AAV5 for treatment of diseases affecting the brain and spinal cord by aiming for a larger area of transduction. As shown in the previous experiment, ICV administration in rats leads to broad transduction of the cerebral areas and spinal cord on DNA and RNA level. To assess the maximum capability of
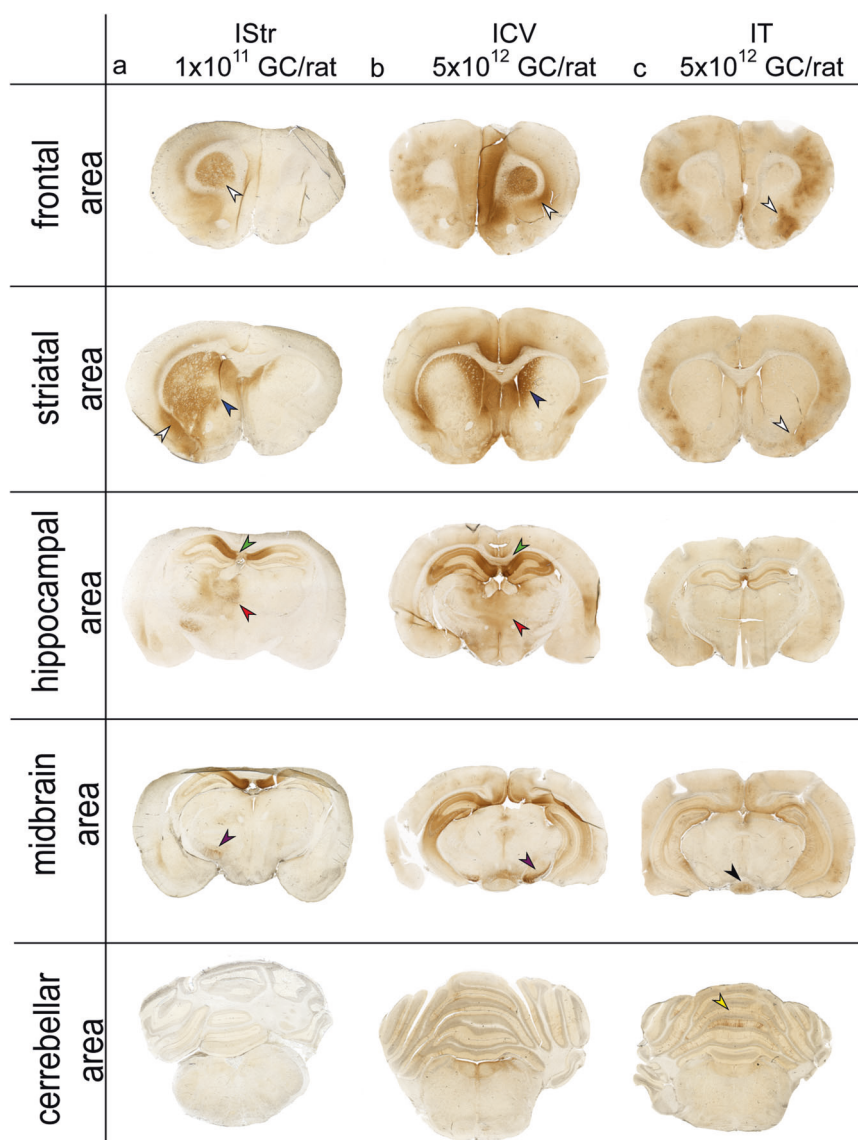
Fig. 3 GFP expression throughout the rat brain following intrastriatal (IStr), intracerebroventricular (ICV), or intrathecal (IT) administration of AAV5-GFP. Rats ($n = 3$) were administered with AAV5-GFP at 1×10^{14} GC/ml, respectively 1, 50, and 50 µl and sacrificed after one month. Brains were extracted, fixed in 4% paraformaldehyde, embedded in gelatin and serially cut with a vibratome to 50 µm sections. **a** IS-administered rats show GFP staining (shown in brown) in the striatum (blue arrow), neocortex (white arrow). Beyond the injection site, also the Cornu Ammonis 1 field of the hippocampus (green arrow), rostral part of the thalamus (red arrow) and the substantia nigra (purple arrow) were positive for GFP signal. **b** ICV-administered rats showed partial GFP IR in the striatal area(blue arrow) and neocortex (white arrow), rostral part of the thalamus (red arrow), the complete hippocampus (green arrow) and the substantia nigra(purple arrow). **c** IT-administered rats showed primarily transduction of the neocortex (white arrows) and hypothalamus (black arrow), and some layers of the cerebellum (yellow arrow). At this magnification level, staining was not observed in the basal ganglia or thalamus. Areas of interest indicated by white arrows. Figure is representative from three animals.

AAV5, the vector was administered ICV and IT (Fig. 1) at the highest titer available, 1×10^{14} GC/ml, and compared to IStr administration as a local and most anterior route of interest. This way the maximum possible spread of the capsid could be analyzed. Administration routed were compared at the same titer, but the volume was adjusted depending on the administration method.

Figure 3 gives an overview of the results following the three administration routes in rat brain. In the frontal area, both IStr (Fig. 3a) and ICV (Fig. 3b) administration of AAV5-GFP resulted in GFP expression in the striatum and the cortex. At this magnification level, staining was only observed in the cortex of IT-administered rats (Fig. 3c). In the striatal area of IStr-injected rats, the striatal area was
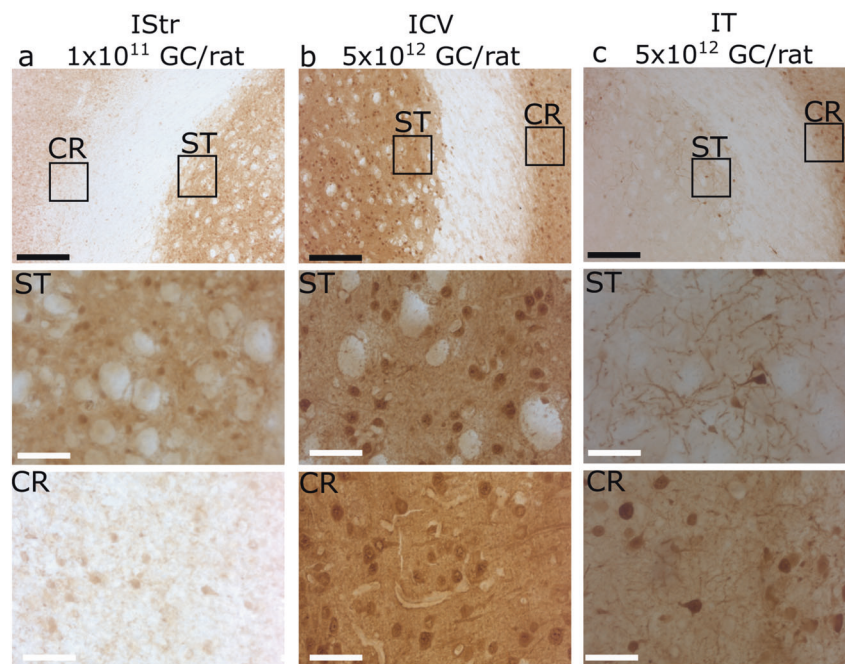
Fig. 4 GFP expression in cortex and striatum in rat brain following intrastriatal (IStr), intracerebroventricular (ICV), or intrathecal (IT) administration of AAV5-GFP. Overview of striatal (ST) and cortical (CR) area from **a** IStr administered rat, **b** ICV administered rats, **c** IT administered rats. Both IStr- and ICV-administration in rats result in GFP stained neurons and the surrounding fibers in the ST area. Striatal area of IT administered rats displayed GFP staining neurons and neurites. However, no GFP staining was observed in the surrounding area. In the cortical area a similar transduction pattern is seen in IT- and ICV-administered rats. In the cortical area of IS-administered rats, the matter staining is less intense compared to the other routes of injection. Black bar represents 1 mm and white bar represents 100 μm for scale.

transduced. In comparison, GFP staining was concentrated around the ventricles surrounding the striatum and the cortex in the brains of ICV-administered rats.

In the hippocampal structure of IStr-administered rats, only the Cornu Ammonis (CA)1 area showed GFP expression. In ICV-administered rats, the complete hippocampal structure appeared to be transduced. IT-administration showed propensity toward a low degree of GFP expression in the molecular layer of the hippocampus. The thalamic area is also positive for GFP staining following IStr and ICV administration.

In the midbrain area, both ICV- and IStr-administered rats displayed GFP staining in the SN, while this area was negative in IT rats. The hypothalamus show some GFP-positive staining in both the ICV and IT administered rats. At the occipital end of the cerebral area, the cerebellum of ICV- and IT-injected rats appeared to have some GFP-positive areas (Fig. 3c)

IT, IS, and ICV administration of AAV5 leads to different GFP expression profiles in the frontal area

Upon taking a closer look at the frontal brain area, we observed a striking difference between the three injection routes. In the striatum of IStr-injected rats, neurons and surrounding matter were GFP positive (Fig.4a, ST). In the cortical area of these rats, GFP-positive neurons were observed, yet the intensity of staining in the surrounding area was less intense compared to that in rats injected in the ICV or IT (Fig. 4a, CR). In ICV-administered rats, the frontal area showed GFP expression in neurons and surrounding matter in the striatum and cortex (Fig. 4b). In the striatum of IT-administered rats positive neurons and axons are observed, however surrounding striatal white matter showed no GFP expression. This is in contrast to pattern seen in ICV- and IStr-administered rats, where the white matter does show transduction (Fig. 4c)

ICV administration of AAV5-GFP leads to GFP expression in the hippocampal and thalamic structure of rats

IStr administration of AAV5-GFP in rats led to GFP staining of the hippocampal layers within the CA1 area, such as the pyramidal cell, lacunosum molecular and oriens layers. Based on their appearance these cells were identified as neurons. Some sparse neurons of the CA2 showed positive staining, but most of this area was negative. Neurons of the CA3 pyramidal cell layer were GFP positive as well as neurons and dendrites in the Dentate Gyrus (DG),

Fig. 5 GFP expression in the hippocampal area in rat brain intrastriatal (IStr), intracerebroventricular (ICV), or intrathecal (IT) administration of AAV5-GFP. a IS-administered rat, b ICV-administered rats, c IT-administered rats. Dentate gyrus (DG) of ICV-administered rats showed GFP staining in the Hilus area which was not seen in the other administration routes. The IStr-administrated animals show GFP stained neurons in the inner molecular area compared to the ICV where the complete CA2 showed GFP staining. Intrathecal (IT)-administered rats had sparse transduction of neurons. In the Thalamic (Th) area, both IStr- and ICV-administered rats showed GFP staining in the thalamic area of neurons and surrounding area. IT administration resulted in GFP stained neurons, however not in the surrounding area. In the overview, Cornu Ammonis (CA)1 is shown. Black bar represents 1 mm scale and white bar represents 100 μm scale.
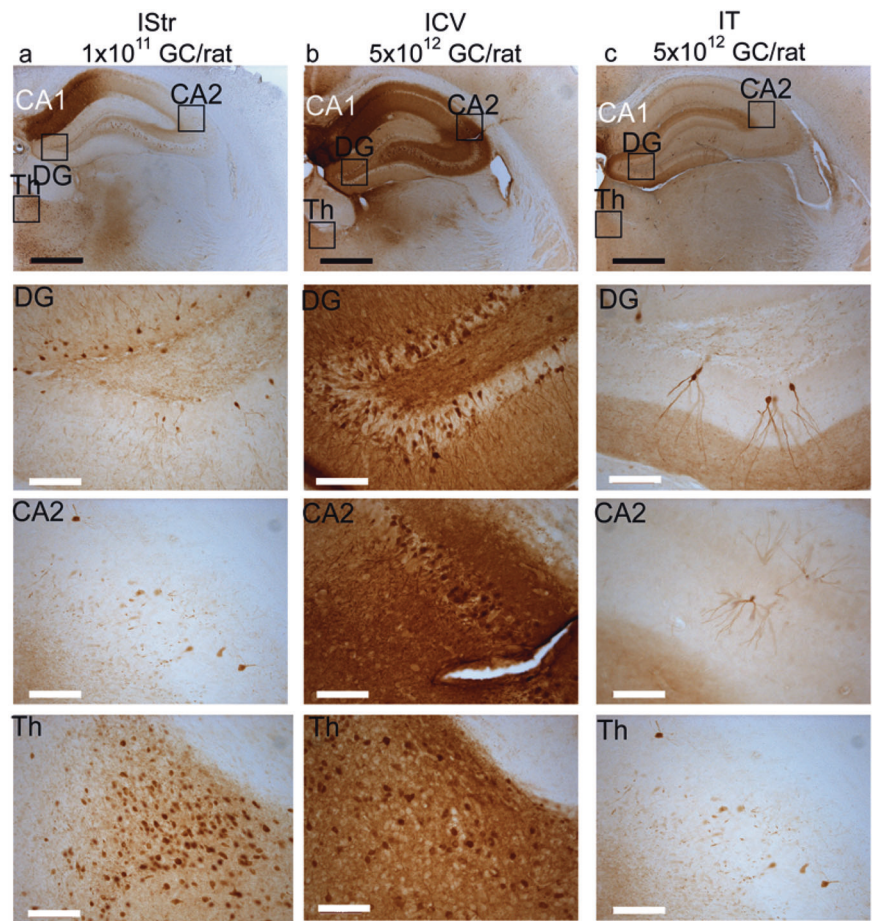
but the surrounding matter and layers of the DG were negative for GFP expression. In the Thalamic (indicated by Th) area, IStr- administered rats showed GFP staining in the thalamic area of neurons and surrounding area (Fig. 5a).

In the ICV-administered rats, the core area of the hippocampus was thoroughly transduced, aiding in clear visualization of its structural architecture. For instance, at the transition from CA1 to CA2, a difference was observed in the intensity of GFP staining. Also, a clear distinction could be made in the morphology of the pyramidal layer of CA2 versus CA1. In the DG neurons of the granular layer were GFP positive as well as surrounding matter and molecular layers. GFP positive neurons and surrounding area could be observed in the thalamic area (Fig. 5b).

In IT-administered rats, strong GFP staining of middle and outer molecular layer of the DG was observed. Positive neurons, dendrites, and axons could be observed in the granular layer of the DG. The morphology of stained cells in the granular layer differs from that of ICV injected rats. In the ICV administered DG, a tightly packed layer of cells was seen, whilst the IT injected neurons were spaced with longer neurites Therefore, it seems that these neurons are in the subgranular zone rather than the granular layer itself. In the CA2 layer multipolar neurons

were seen with branching dendrites. However, the layers themselves were negative for GFP staining (Fig. 5c).

Altogether, the results suggest that depending on the injection route AAV-mediated transduction patterns involve different hippocampal and/or thalamic neuronal pathways.

IT, IStr, and ICV administration of AAV5 results in different GFP- expression profiles in SNpc hypothalamus and cerebellum of rats

In the midbrain area, the SN pars compacta (SNpc) and pars recticulata (SNrc) as well as in the ventral tegmental area (VTA), several neurons were positive for GFP in brains of IStr-administered rats. All other areas of the midbrain were negative (Fig. 6a). After ICV injection, the SNrc and VTA are positive for GFP but not the SNpc. In the medial mammillary body of the hypothalamus GFP positive neurons are perceived (Fig. 6b).

In brains from IT-administered rats, predominantly cells of the mammillary body were positive for GFP (Fig. 6c). In the cerebellum of IStr-administered rats, no positive neurons could be discerned (Fig. 6d). ICV injection led to sparse transduction of the cerebellum, but positive Purkinje

Fig. 6 GFP staining in the midbrain area and cerebellum in rat brain following intrastriatal (IS), intracerebroventricular (ICV), or intrathecal (IT) administration of AAV5-GFP. **a–c** overview of midbrain area. ×20 magnification of the substantia nigra of IS administrated rats showed GFP stained neurons in the substantia nigra pars compacta (white arrow) and pars reticulata (black arrow), ICV administered rats showed GFP staining in the pars reticulata but not in the pars compacta. In the hypothalamus (hyp) GFP IR neurons were observed in ICV- and IT administered rats for which IStr administered rats are negative. **d–f** In the cerebellum of IT-administered rats, show GFP staining in Purkinje cells(white arrow) and Bergman cells(black arrow). Neuronal staining also found in ICV-administered rats. However, transduced cells are more sporadic as compared to IT administration. No staining observed in IStr- administered rats. Black bar represents 500 μm, white bar 100 μm, and brown bar 50 μm for scale.
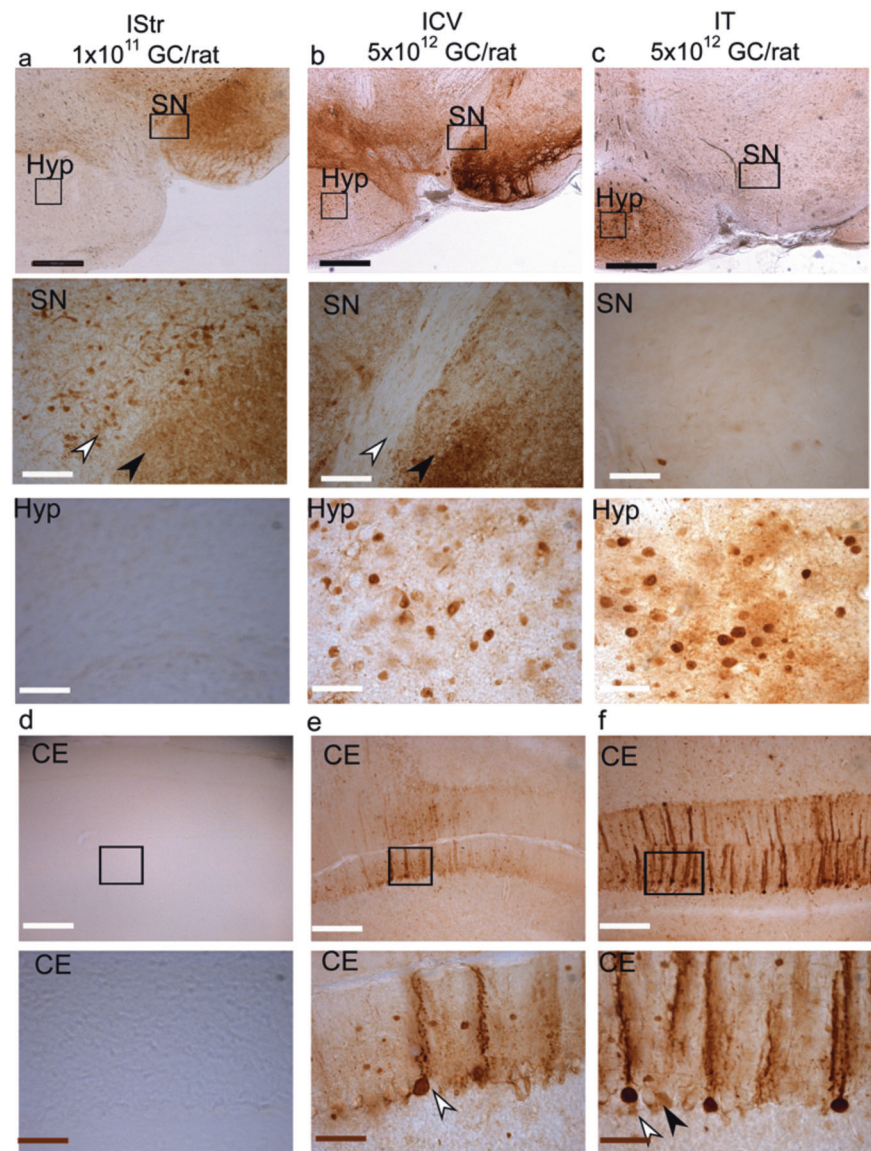
were identified (Fig. 6e, shown by arrow). In the cerebellum of IT-administered rats, more layers with positive cells were identified, for example Purkinje and Bergman Glia cells based on morphology and location (Fig. 6f).

ICV- and IT-administration of AAV5-GFP results in GFP expression in spinal cord and dorsal root ganglia of rats

Along the entire length of the spinal cord (SC) and aligned Dorsal Root Ganglia (DRG) of IStr-administered rats, no GFP-positive cells were observed (not shown). The cervical SC of ICV-injected rats did also not show staining for GFP. However, positive cells were observed in the cervical DRG. These GFP positive large round bodies are assumed to be neurons which are indicated by arrows. In the thoracic area,

sporadic positive neurites in the dorsal root entry zone could be observed in the dorsal horn. Also, GFP-positive neurons in the DRG were observed. At the lowest part of the spinal cord at the lumbar section, GFP-stained neurons were visualized in the DRG (Fig. 7a). IT administration led to positive neurons at the cervical SC but not attached DRG, moving downward to the thoracic section positive cells can also be observed in both SC and DRG. Surprisingly, no GFP positive cells observed in the dorsal horn of the lumbar SC, staining is observed in the lumbar DRG (Fig. 7b).

Discussion

In this study, we show that the distribution profile of AAV in the CNS is highly dependent on its delivery method.

Fig. 7 GFP staining in the spinal cord and the dorsal root ganglion of intracerebroventricular (ICV) and intrathecal (IT) administered AAV5 rats. **a** ICV-administered rats showed staining of cervical DRG, DRG, SC, and lumbar DRG. **b** IT-administered rats show GFP positive cells and matter in cervical SC, thoracic SC&DRG, and lumbar DRG. GFP stained cells marked by Arrow. White bar represents 100 μm and brown bar 50 μm for scale.
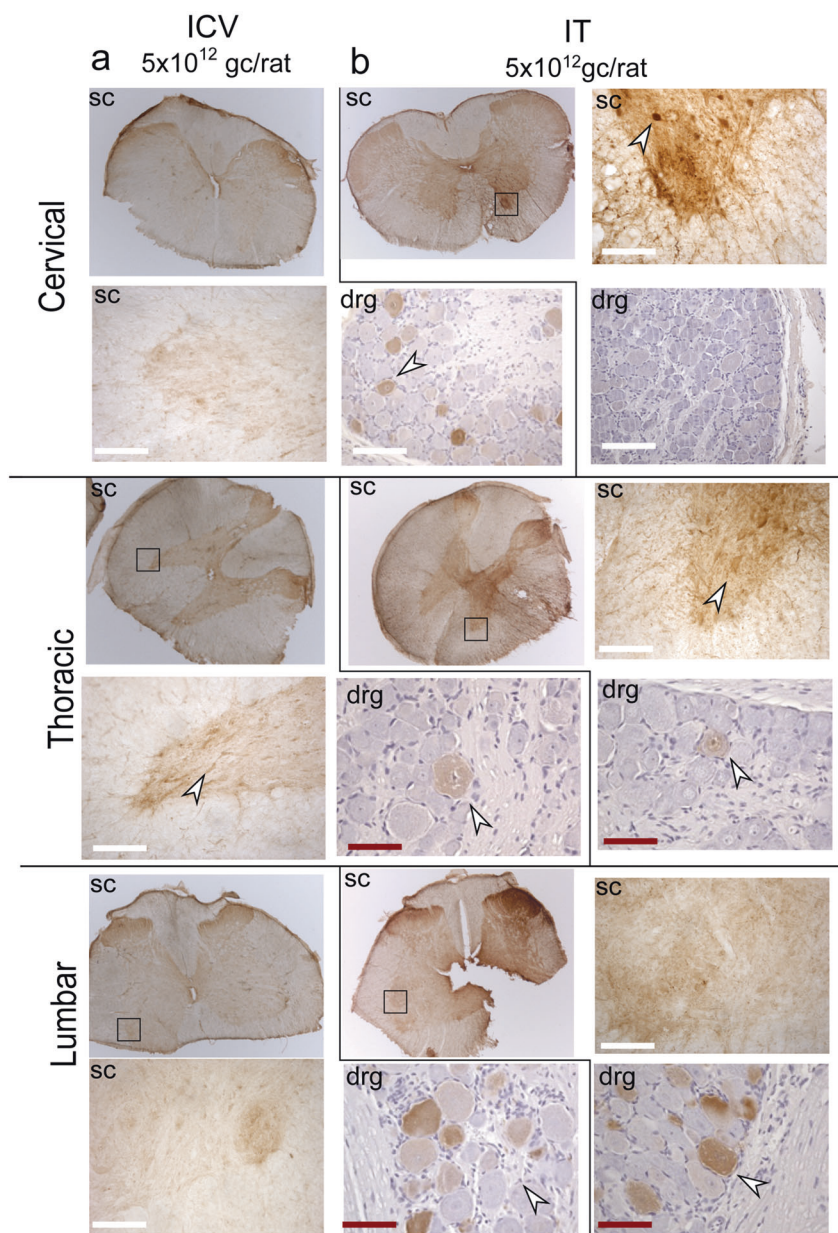
Thus, depending on the disease for which therapy is being developed each method has its own merits. IStr and ITH are more suited for diseases in which a high concentration of therapeutic compound is needed locally in the frontal to mid brain areas, such as PD and HD. ICV is suited for low to mid-range transgene delivery in a broad distribution throughout the CNS with somewhat less penetration into deeper brain structures but could be useful for e.g., lysosomal storage diseases.

The question whether AAV5 is specific for neurons or glial cells is not addressed in this study. Neurons and glial cells however, can be identified by their characteristic shape. The scope of this study has not been to quantify the ratio of transduced neurons and glial cells but rather the

transduction pattern in general. Moreover, based on location, one could identify neuronal cell bodies if they are at relative long distance from the injection site as a result from anterograde or retrograde transduction [8].

In brains of IStr-administered rats, vector and transgene expression were detected in the thalamus, cortex, and hippocampus, and thus outside the injected nucleus. There are strong indications that AAV travels beyond the injection site by axonal transport [13]. Following IStr administration of AAV5 in NHP, AAV5 transduced the SNpc, cortex, and thalamus by retrograde transduction and SNpr by anterograde transduction [8]. Anterograde transport is characterized by transduction of vector distal to the injection site after cell body-mediated uptake. Retrograde transport

involves the uptake of viral particles by nerve terminals at the site of injection, which are then transported to the cell body of the neuron. Samaranch et al. [8] showed the same pattern of GFP-positive nuclei in NHP as we observed in rats. Therefore, in rats as well as NHP AAV5 may well use the same anterograde and retrograde mode of transport. This has great implications for the capability to predict the transduction patterns across species.

While ICV is a less invasive and simpler surgical procedure, ICV administration only targets the SNpr and not the SNpc. In an earlier study comparing IStr- to ITH-delivery in NHP, it was also observed that ITH delivery does not result in the transduction of the SNpc whilst IStr administration does. [8]. These results suggest that of the delivery methods studied for PD, IStr administration of AAV5-based therapy is currently the best option to deliver meaningful amounts of therapeutic to neurons of the SNpc. As an additional transduction area to the SN, parts of the hippocampus are transduced. Depending on the therapeutic target, this spread could either have an added value or something to carefully evaluate.

Our distribution analysis showed that vector copies were detected evenly across all tissues analyzed following ICV infusion of AAV5. In contrast to direct infusion into the striatum, where almost the complete area was GFP positive, only the nuclei in the vicinity of the lateral ventricle were positive for GFP after ICV administration. However, ICV injection led to complete transduction of the hippocampus making this a feasible alternative to direct administration into the hippocampal formation. Obtaining this knowledge is crucial for the development of AAV-based therapies for AD.

The SNpr, cerebellum and spinal cord could be transduced via the subarachnoid space. During the systolic phase, CSF flows from the ventricles into the subarachnoid space and spinal cord via the foramen located below the cerebellum. The SNpr projects to the thalamus, resulting in retrograde transduction of the thalamus when transduced with AAV5. The thalamus has an afferent projection to the mammillary body which could explain the positive cells observed in this region. Based on the transduction pattern it seems that ICV-based-AAV5 transduction of the brain is a mixture of transependymal CSF flow of structures close to the ventricles and subsequent axonal transport to deeper areas. The transependymal CSF flow describes the progress of CSF across the ependymal layer that surrounds the ventricles into the brain parenchyma and adjacent structures. This flow is pushed by a pressure gradient which is driven by the production of CSF in the lateral ventricles. CSF flows in the direction of the venous sinuses into which it is eventually absorbed [20].

Lumbar IT delivery of AAV5-GFP resulted in GFP-positive cells in SC and DRG. Some GFP-positive neurons were also observed in the cerebrum, the cerebellum and frontal brain. There are indications that after IT administration AAV9 and AAVrh10 transduce the parenchyma via perivascular transport of CSF [21, 22]. It is feasible that AAV5 uses the same mechanism to cross the pia mater. Guo et al. [22] observed distinct GFP patches in the vicinity of vascular cavities in rat brains following IT administration of AAVrh10 and double staining with aquaporin 4, a marker for perivascular space, showed colocalization with GFP expression. We did not observe an obvious pattern of colocalization of vascular cavities and GFP staining after AAV5 administration. Both AAV9 and AAVrh10 are known to cross the blood-brain barrier after IV administration, while AAV5 does not [10], indicating that AAV5 employs a different method to cross pia mater.

Even though in both IT and ICV the same amount of vector is administered to the CSF, a different expression pattern was observed. For example, in the striatum of IT administered rats neuronal and axonal staining is observed, indicating that a different set of neurons seem to be transduced in the striatum when infused intrathecally when compared to ICV. One possible explanation for this observation is the flow of the CSF. ICV-administered vector moves with the natural flow of the fluid, from the lateral ventricle, where CSF is produced, to ventricles beyond. AAV5 injected into the lumbar subarachnoid space has to populate and transduce the tissue against the flow and has no gradient push toward the parenchyma of the cerebrum. This make it difficult for the vector to transduce cells in the cerebrum via CSF after IT administration. The GFP-positive areas observed in the cerebrum after IT administration are most likely due to axonal transport rather than transport of the vector via the CSF. We hypothesize that for successful transduction of striatal neurons, a specific threshold needs to be reached to obtain sufficient vector spread. Therefore, also concentration of the vector at a certain location may be decisive for its ability to transduce a certain set of cells or brain areas.

Surprisingly, ITH- and ICV-administered vector was observed outside the CNS, however this did not result in GFP-RNA expression. Possibly, the CAG promoter was not active in rats in these organs. In a study using the CAG promoter in a non-human primate (NHP) vector, the distribution in the periphery also did not lead to expression in the spleen, kidney, and liver [23]. Surprisingly, the CAG promoter is active in mouse liver [24], pointing towards species specificity of the promoter in peripheral organs. Presence of vector copies in unwanted locations may lead to side effects. In that case, the use of a CNS specific promoter could be considered.

On the other hand, the delivery methods targeting all tissues equally are advantageous for lysosomal diseases such as Mucopolysaccharidoses IIA, where both the organs

of the periphery and the CNS are affected. Both IT-and ICV-delivery routes can be considered for the treatment of such diseases that need a widespread transduction. Furthermore, lysosomal enzymes are capable of cross-correction as they are secreted to the extracellular space and taken up by neighboring cells which were not transduced, and have the capacity to travel across axonal projections [25]. Due to these properties, the IT- and ICV-induced transduction to distal areas may give a therapeutic effect.

To allow translation to humans, the delivery methods should be tested in larger animal models. IStr administration of AAV5 has been tested in numerous NHP studies [6, 8, 26]. IT delivery of AAV5 was tested in NHP at the same dose as in the current study and a similar transduction pattern was observed [8]. Of the delivery methods, ICV is the least tested in larger animal models, but in dogs resulted in efficient transduction of the brain and spinal cord, and, importantly, no adverse effects were seen [27]. In a more recent study, ICV administration to the lateral ventricle of dogs resulted in encephalitis in one animal [14]. As ventriculostomy is a common procedure in humans, one would not suspect the procedure to be high risk. However, both represent small studies and more research on large-animal preclinical models for ICV administration is necessary to carefully assess this delivery method and compare it to alternative methods. Overall, we believe that some common mechanisms that use anatomical features are present in both rodents and larger animals, such as striatal connections to SN or cortex. Therefore, studies can be better tailored to include retrograde and anterograde transduction mechanism patterns.

Based on our current data and data from others, IStr and ITH could be used for gene-delivery therapy for more localized diseases such as PD and HD. ICV could be employed for a disease like AD targeting the hippocampus and due to its broader reach also AAV5-based therapy for lysosomal storage disease could be developed using ICV delivery. Both ICV and IT could be used for diseases where the cerebellum is the main target, although the transgene expression levels are relatively low. Moreover, IT delivery of AAV5-mediated therapy transduces the complete spinal cord and most of the cortical area, and could thus be used for diseases affecting the spinal cord.

This study was performed in rodents and therefore the delivery methods need to be studied in larger animal models prior to application in the clinic. Ongoing studies in both wild-type and transgenic HD minipigs show promising results for IStr- and/or ITH-administration to HD-patients [28]. Especially when degeneration of the striatum is advanced, thalamic infusion may be an attractive alternate option. Our current data constitute a solid base for further development of AAV5-based gene therapy for neurological diseases.

Compliance with ethical standards

Conflict of interest The authors declare that they have no conflict of interest.

Publisher's note Springer Nature remains neutral with regard to jurisdictional claims in published maps and institutional affiliations.

References

1. Leone P, Shera D, McPhee S, Francis JS, Kolodny EH, Bilaniuk LT, et al. Long-term follow-up after gene therapy for canavan disease. Sci Transl Med. 2012;4:165ra163–165ra163.
2. Boutin S, Monteilhet V, Veron P, Leborgne C, Benveniste O, Montus M, et al. Prevalence of serum IgG and neutralizing factors against adeno-associated virus (aav) types 1, 2, 5, 6, 8, and 9 in the healthy population: implications for gene therapy using AAV vectors. Hum Gene Ther. 2010;21:704–12.
3. Aschauer DF, Kreuz S, Rumpel S. Analysis of transduction efficiency, tropism and axonal transport of AAV serotypes 1, 2, 5, 6, 8 and 9 in the mouse brain. PloS ONE. 2013;8:e76310.
4. Lisowski L, Tay S, Alexander I. Adeno-associated virus serotypes for gene therapeutics. Curr Opin Pharmacol. 2015;24:59–67.
5. Paterna J-C, Feldon J, Büeler H. Transduction profiles of recombinant adeno-associated virus vectors derived from serotypes 2 and 5 in the nigrostriatal system of rats. J Virol. 2004;78:6808–17.
6. Dodiya HB, Bjorklund T III, J Mandel RJ, Kirik D, Kordower JH. Differential transduction following basal ganglia administration of distinct pseudotyped AAV capsid serotypes in nonhuman primates. Mol Ther. 2010;18:579–87.
7. Markakis EA, Vives KP, Bober J, Leichtle S, Leranth C, Beecham J, et al. Comparative transduction efficiency of AAV vector serotypes 1–6 in the substantia nigra and striatum of the primate brain. Mol Ther. 2010;18:588–93.
8. Samaranch L, Blits B, Sebastian SW, Hadaczek P, Bringas J, Sudhakar V, et al. MR-guided parenchymal delivery of adeno-associated viral vector serotype 5 in non-human primate brain. Gene Ther. 2017;24:253–61.
9. Martier R, Liefhebber JM, García-Osta A, Miniarikova J, Cuadrado-Tejedor M, Espelosin M, et al. Targeting RNA-mediated toxicity in C9ORF72 ALS/FTD by RNAi-based gene therapy. Mol Ther—Nucleic Acids. 2019;16:26–37.
10. Schuster DJ, Belur LR, Riedl MS, Schnell SA, Podetz-Pedersen KM, Kitto KF, et al. Supraspinal gene transfer by intrathecal adeno-associated virus serotype 5. Front Neuroanat. 2014;8:66.
11. Schapira A, Chiasserini D, Beccari T, Parnetti L. Glucocerebrosidase in Parkinson's disease: insights into pathogenesis and prospects for treatment. Movement Disord. 2016;31:830–5.
12. Reiner A, Dragatsis I, Dietrich P.Genetics and neuropathology of Huntington's disease. Int Rev Neurobiol. 2011;98:325–72.
13. Salegio E, Samaranch L, Kells A, Mittermeyer G, Sebastian SW, Zhou S, et al. Axonal transport of adeno-associated viral vectors is serotype-dependent. Gene Ther. 2012;20:gt201227.
14. Furman JL, ma D, Gant JC, Beckett TL, Murphy PM, Bachstetter AD, et al. Targeting astrocytes ameliorates neurologic changes in

a mouse model of Alzheimer's disease. J Neurosci. 2012;32:16129–40.

15. Hardcastle N, Boulis NM, Federici T. AAV gene delivery to the spinal cord: serotypes, methods, candidate diseases, and clinical trials. Exp Opin Biol Ther. 2017;18:1–15.

16. Tardieu M, Zérah M, Gougeon M-L, Ausseil J, de Bournonville S, Husson B, et al. Intracerebral gene therapy in children with mucopolysaccharidosis type IIIB syndrome: an uncontrolled phase 1/2 clinical trial. Lancet Neurol. 2017. https://doi.org/10.1016/s1474-4422(17)30169-2.

17. Bosma B, du Plessis F, Ehlert E, Nijmeijer B, de Haan M, Petry H, et al. Optimization of viral protein ratios for production of rAAV serotype 5 in the baculovirus system. Gene Ther. 2018;25:415–24.

18. Oudega M, Varon S, Hagg T. Regeneration of adult rat sensory axons into intraspinal nerve grafts: promoting effects of conditioning lesion and graft predegeneration. Exp Neurol. 1994;129:194–206.

19. Gray SJ, Foti SB, Schwartz JW, Bachaboina L, Taylor-Blake B, Coleman J, et al. Optimizing promoters for recombinant adeno-associated virus-mediated gene expression in the peripheral and central nervous system using self-complementary vectors. Hum Gene Ther. 2011;22:1143–53.

20. Casaca-Carreira J, Temel Y, Hescham S-A, Jahanshahi A. Transependymal cerebrospinal fluid flow: opportunity for drug delivery? Mol Neurobiol. 2018;55:2780–8.

21. Schuster DJ, Dykstra JA, Riedl MS, Kitto KF, Belur LR, McIvor SR, et al. Biodistribution of adeno-associated virus serotype 9 (AAV9) vector after intrathecal and intravenous delivery in mouse. Front Neuroanat. 2014;8:42.

22. Guo Y, Wang D, Qiao T, Yang C, Su Q, Gao G, et al. A single injection of recombinant adeno-associated virus into the lumbar cistern delivers transgene expression throughout the whole spinal cord. Mol Neurobiol. 2016;53:3235–48.

23. Meyer K, Ferraiuolo L, Schmelzer L, Braun L, McGovern V, Likhite S, et al. Improving single injection CSF delivery of AAV9-mediated gene therapy for SMA: a dose–response study in mice and nonhuman primates. Mol Ther. 2015;23:477–87.

24. Chen B, He C, Chen X, Pan S, Liu F, Ma X, et al. Targeting transgene to the heart and liver with AAV9 by different promoters. Clin Exp Pharmacol Physiol. 2015;42:1108–17.

25. Cearley CN, Wolfe JH. Transduction characteristics of adeno-associated virus vectors expressing cap serotypes 7, 8, 9, and Rh10 in the mouse brain. Mol Ther. 2006;13:528–37.

26. Emborg ME, Hurley SA, Joers V, Tromp DPM, Swanson CR, Ohshima-Hosoyama S, et al. Titer and product affect the distribution of gene expression after intraputaminal convection-enhanced delivery. Stereotactic Funct Neurosurg. 2014;92:182–94.

27. Haurigot V, Marcó S, Ribera A, Garcia M, Ruzo A, Villacampa P, et al. Whole body correction of mucopolysaccharidosis IIIA by intracerebrospinal fluid gene therapy. J Clin Investig. 2013;123:3254–71.

28. Evers MM, Miniarikova J, Juhas S, Vallès A, Bohuslavova B, Juhasova J. et al. AAV5-miHTT gene therapy demonstrates broad distribution and strong human mutant huntingtin lowering in a Huntington disease minipig model. Mol Ther. 2018;26:2163–77.